sensors

Article

Estimation of chlorophyll a concentration in tropical wetlands with sentinel 2 images implementing machine learning.

Cesar Padilla-Mendoza [1]*, ORCID: 0000-0002-1777-9730

[1] Universidad Nacional de Colombia; cpadillam@unal.edu.co
* Correspondence: cpadillam@unal.edu.co;

Abstract: The Sentinel 2 mission provides medium resolution images, which can be used to subsequently map chlorophyll a (Chl a) concentrations in inland water bodies. In this research, two machine learning techniques called ensemble methods and multiple linear regression (MLR) were used to estimate Chl a based-on Sentinel 2 imagery for a tropical wetland in northern Colombia. This model was validated by linking reflectance values with in situ Chl a data synchronous to the Sentinel 2 image dated December 07, 2021 (N = 80). The Multiple Linear Regression model showed regular results (R2 = 0.482, RMSE = 0.0063, MAE=0.070), however, in its model it takes into account the infrared, green and red bands, which captures this parameter; the ensemble method presented better results with the same bands (R2 = 0.623, RMSE = 0.0004, MAE=0.002). So these machine learning techniques work well for Chl a and information from remote areas can be known.

Keywords: Chlorophyll a ; Machine learning; tropical wetland

1. Introduction

Eutrophication is a problem that has occurred in tropical wetlands, affecting the surrounding ecological environment [1]. To study such a problem, chlorophyll a, which is useful to estimate also phytoplankton biomass, has been taken into account. Remote sensing technology has been combined with field-synchronized data for the quantitative calculation of water quality parameters [2]. Data from medium resolution satellite images such as Sentinel 2 have shown great potential for quantitative detection of chlorophyll a in water [3,4]. Due to the free availability of Sentinel 2 images, they have become a tool in water quality monitoring.

Previous studies have evaluated surface water quality in the Ciénaga Grande del Bajo del Sinú by observing water physicochemical parameters (WQP). [5] combined conventional field methods with the use of remote sensing (RS) to estimate the concentrations of dissolved oxygen, temperature, turbidity, conductivity, pH and total dissolved solids, from empirical models implementing multiple linear regression, and finally represent the results in concentration maps of each parameter.

Sentinel-2 reflectance values have provided accurate estimates of water quality parameters, in different tropical areas such as Brazil [6], China [7] and Africa [8]. However, it is observed that the models obtained from reflectance vary depending on the location and modeling technique, hence, they are results with mixed accuracies [9].

Machine learning models such as Random Forest, Suppot Vector Machine, neural networks, etc., have been shown to provide better accuracies due to their ability to automatically learn from data, explain hidden patterns and nonlinearity in reflectance data and chlorophyll a as an optically active parameter [10, 11, 12]. Therefore, the resolution of satellite image data and modeling technique are fundamental to implement updated monitoring for the Lower Sinu Marsh, the robustness of the model can provide reliable point estimates and spatio-temporal mapping of chlorophyll-a. The objective of this study

Citation: To be added by editorial staff during production.

Academic Editor: Firstname Lastname

Received: 08/12/2022
Accepted: date
Published: date

Publisher's Note: MDPI stays neutral with regard to jurisdictional claims in published maps and institutional affiliations.

is to estimate chlorophyll a in a tropical wetland based on reflectance models. To achieve this, the performance of two statistical models (ensembles and linear regression) was evaluated on chlorophyll a data of the Ciénaga Grande del Bajo Sinú from Sentinel 2 satellite images.

2. Materials and Methods

2.1. Study area

The Bajo Sinú swamp complex is located in the north of the department of Córdoba, Colombia. This system receives contributions from the Aguas Prietas and Bugre streams and some direct contributions from the Sinú River during the rainy season. The complex was declared a protected area by the local environmental authority because of its ecological and economic importance [13].

The research was carried out specifically in the Bajo Sinú swamp complex, which is formed mainly by the Guartinaja, Sapal and Momil swamps, which at the time of sampling had areas of 27.10 km^2 , 2.96 km^2 and 6.63 km^2 respectively. For the monitoring, 80 stations were distributed in the marshes, 58 in Guartinaja, 9 in Sapal and 13 in Momil (Figure 1).

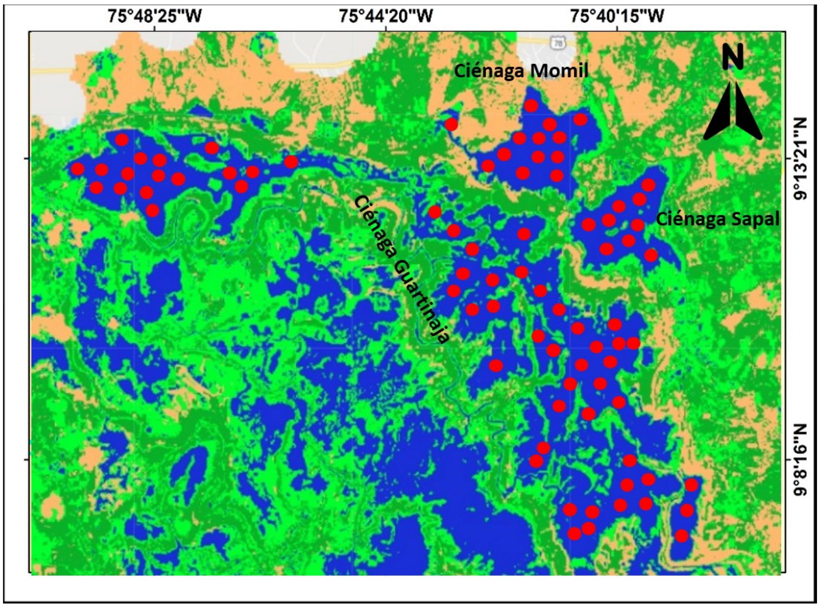

Figure 1. Location map of study area

2.2. In situ data

Water quality sampling was conducted on December 07, 2021, synchronously with Sentinel 2A passing over the swamp complex and 80 samples were collected. Chlorophyll a was analyzed in the laboratory using a glass fiber filter to filter the water and then soaked in 90% acetone to extract the pigments [14]. The light absorbance of the extracted solution was measured at 630 (A630), 645 (A645), 663 (A663) and 750 nm (A750) using a UV2600 spectrophotometer [15]. Chlorophyll-a values were then obtained for each sample.

2.3. Satellite data acquisition

Sentinel 2 satellite images were used to estimate chlorophyll a in the bog. An image with a minimum cloudiness of less than 10 % was used, covering the spatial extent of the bog and corresponding to the field water sampling period. Level 2A data products were freely obtained from the Copernicus Open Access Hub platform of the European Union (https://scihub.copernicus.eu/) [16]. The date of access to the dataset was 07 December 2021.

2.4. Modelling the relationship between measured Chlorophyll-a and spectral values

To determine the patterns between measured chlorophyll a values and remote sensing spectral values for the bog, two regression models were applied; a parametric multiple linear regression (MLR) and ensemble models based on Random Forest.

2.4.1. Multiple linear regression

To fit the MLR models, standard assumptions underlying linear regression analyses were evaluated based on tests of normality and variance homogeneity for each response variable using the Shapiro-Wilk test in Python, respectively. To avoid the issues of multicollinearity among the predictors, we used the information from both the Pearson product moment of correlation coefficient (r) and the variance inflation method (VIF) to remove highly correlated predictors[18]. The MLR was fitted by the ordinary least squares method and was implicitly expressed as:

$$Y = \beta_0 + \beta_1 X_1 + \beta_2 X_2 + \cdots + \beta_P X_P + \varepsilon \quad (1)$$

Where Y is the (response variable); β_0, $\beta_1, \beta_2, \cdots, \beta_P$ denote the regression parameters to be estimated; X_1, X_2, X_P are the remotely-sensed spectral bands; and ε is the independent and identically distributed errors with an expectation, $\mathrm{E}(\varepsilon) = 0$ and a constant variance, $Var(\varepsilon) = \sigma^2$.

The significance of model parameters was tested at both 1% and 5% probability levels. During the MLR model fitting, predictors were included into the model by a stepwise approach (both 'forward and backward' selection) using the base packages of 'caret' and 'MASS' in R to enhance best model performance by lowering the estimation error[19].

2.4.1. Random forests

RF is a supervised ensemble-learning algorithm which has shown higher predictive performance in classification and regression analyses [20]. RF works by generating a set of decision trees that are aggregated to reduce the variance of predictions (i.e. overfitting). Among the predictor variables, the RF model was optimized by hyper-parameter tuning following similar procedures described by [21], [22]. The RF model was fitted in python using the "RandomForestRegressor" library [23].

2.5. Assessment of algorithms

In this study, the algorithms used are assessed using three statistical methods namely coefficient of determination (R2) [24], root mean square error (RMSE) (Moore et al., 2014), and mean absolute error (MAE) [25].

2.6. Obtaining maps

To obtain the concentration map, the bog contour was extracted by applying the NDWI index with the Sentinel 2A image. Subsequently, the empirical model obtained from the linear regression model was used in the QGIS raster calculator, version 3.16, to generate the spatial distribution map of Chlorophyll a [26].

3. Results

3.1. Statistical analysis

The mean and standard deviation (mean ± SD) of chlorophyll a was 19.62 ± 5.37 mg/L with a minimum value of 7.94 mg/L and a maximum of 33.35 mg/L. That is, in all measurement points, the concentrations are within the range of acceptable values for this type of water bodies, however, it is likely to change the trophic condition if there is a greater imbalance of nutrients [27]. Spearman's coefficient results that there is a high relationship between chlorophyll a and bands B8-B3. The data shows a Cauchy type distribution (Figure 2).

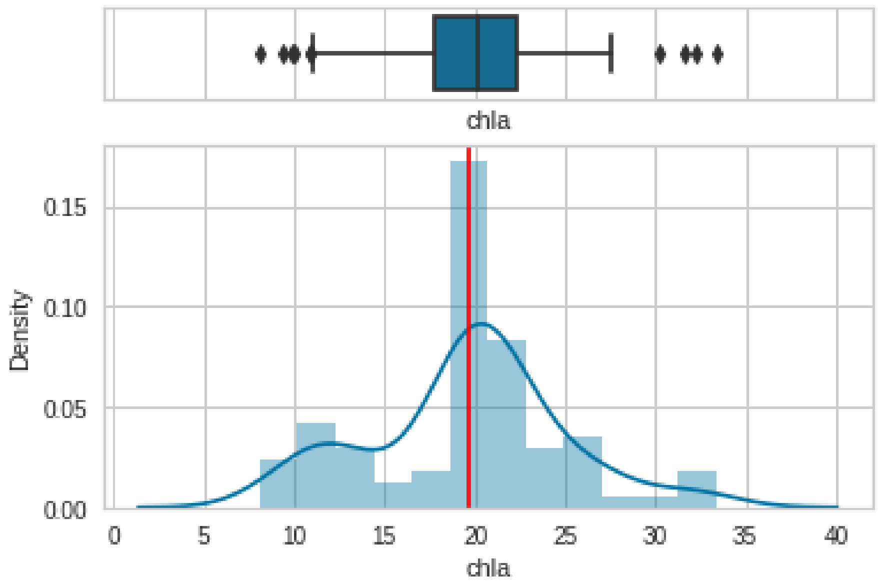

Figure 2. Chlorophyll-a data distribution

The reflectance values presented heterogeneous distributions, however, most of the bands presented asymmetry towards the left, except for bands B4, B5, B3 and B12.

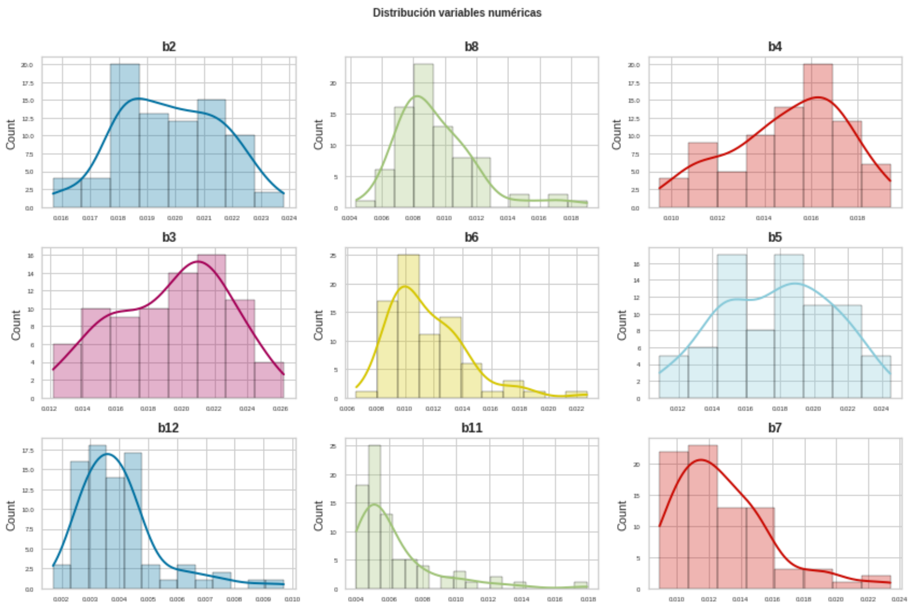

Figure 3. Spectral values data distribution

3.2. Regression analysis for obtaining models

3.2.1. Multiple linear regression

The multiple linear regression showed that the most representative bands in the model are B8, B5, B3, B2 and B12, all the bands taken into account by the model are reported in literature to estimate chlorophyll a [28], however B12 is not commonly found within this group, it may be associated with fluctuations or accumulated errors. Here in this method the R2 was 0.48 and the MAE was 0.07, these values of the evaluation coefficients are not significant for this type of processes, so it is not recommended to make estimations.

Table 1. Linear regression model.

Term	Coefficient
Log [Chl_A]	
Intercept	1.282860
B8	-0.37136214
B8/B3	0.07554
B5*B8	0.29807
B2*B12	0.0110
B3/B8	-0.07444

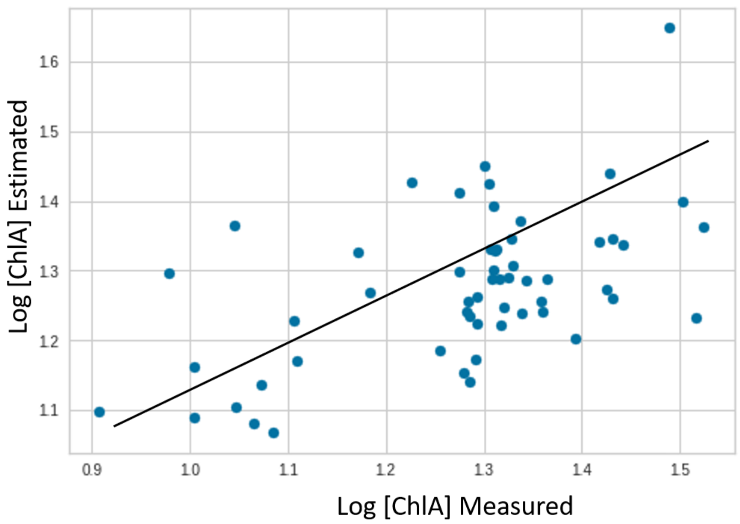

Figure 4. Measured vs estimated

3.2.2. Ensemble models based on Random Forest

The assembled models based on random forest obtained an R2 of 0.623, RSME = 0.0004 and MAE = 0.002, this method proved to be more efficient than linear regression, however, it has the disadvantage that the coefficients of each independent variable are unknown, therefore, estimates cannot be made with raster, however, this method allows capturing nonlinearities that are generated between the variables [29].

3.3. Chlorophyll a concentration map

The multiple linear regression algorithm and ensemble model trained with 70% of the in situ Chl a data showed unsatisfactory performance. These algorithms provide the ability to estimate Chl a in tropical wetlands, with the multiple linear regression algorithm being more useful for obtaining concentration maps. The model obtained from this method shows that Chl a in the central zones of the Guartinaja marsh, present homogeneous distributions with intermediate values, the predominant concentrations are between 12 and 16 mg/L. This corresponds appropriately to the field measurement, since the water body presents eutrophication processes. For the Momil and Sapal bogs, there is less uniformity of chlorophyll a concentration, with Momil showing low values of less than 12 mg/L (Figure 4). We note that one of the disadvantages of the ensemble model is that it does not present the coefficients of the implemented variables, and therefore, for this case, they cannot be represented in raster form.

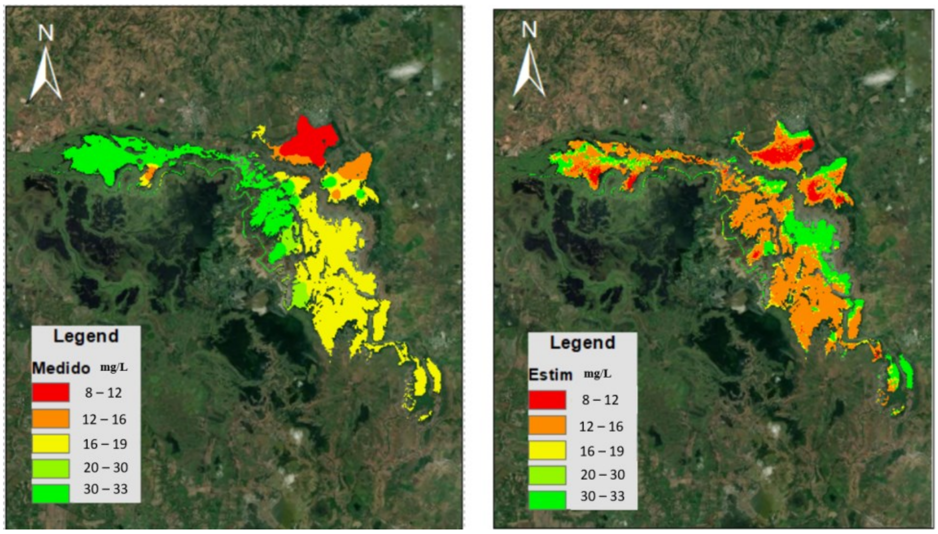

Figure 4. Chlorophyll a concentration map

4. Discussion

The objective of this study was to explore the feasibility of sentinel 2A images for estimating chlorophyll a concentration by implementing two machine learning techniques. The highest accuracies obtained from the models tested indicated that chlorophyll a could be derived from spectral reflectance data. I obtained higher accuracies with the ensemble machine learning (RF) models than with traditional linear regression models. Similarly, using machine learning models, [30], [31] found accuracies of 71 % and 94 % with RF for mapping potential groundwater in Iran and India, respectively. [32], [33] suggested that the overall better performance of machine learning models with reflectance values compared to parametric models is that machine learning models allow discovering nonlinear and higher level statistical relationships. Analyzing the bands selected to find the response variable, these correspond to the combinations of NIR (B8), red (B4 or B5) and green (B3) bands in Sentinel sensors retrieve Chla in some coastal and inland waters [34].The predicted chlorophyll a range was similar to other recent studies conducted in the tropical area [35, 36], but showed increasing trends compared to [37] . However, a similar study is needed for the rainy season to determine the spatio-temporal trends in water quality in the Ciénaga Grande Del Bajo Sinú.

5. Conclusions

Two machine learning algorithms, multiple linear regression and assembled models based on random forest, were implemented to generate empirical models taking into account chlorophyll a and reflectance values from the Sentinel 2A satellite image. The models present low correlation between measured and estimated data; therefore, they work moderately to obtain Chl a concentration distribution maps, useful to identify areas where there are high values and that can induce intense processes of alteration of the natural dynamics of the Lower Sinu swamp complex.

The applied machine learning methods proved to be useful to integrate techniques such as remote sensing combined with traditional water quality monitoring, since the concentration map appropriately represented the real conditions of the studied water body. This technique has its limitations due to climatic conditions; however, given the reduction of time and costs for monitoring these ecosystems, it becomes an integral analysis alternative for the continuous supervision, preservation and possible forms of adaptation of these aquatic ecosystems in the face of climate change.

Cesar David Padilla Mendoza: Conceptualization, methodology, Investigation, Writing – original draft, Writing – review & editing and Funding acquisition.

Acknowledgments: Thanks to Professor Edier Aristizabal for his guidance on machine learning.

References

1. Groot, D.; Brander, L.; Finlayson, M. Wetland Ecosystem Services. In *The Wetland Book*; Finlayson, C.M., Everard, M., Irvine, K., McInnes, R.J., Middleton, B.A., van Dam, A.A., Davidson, N.C., Eds.; Springer Netherlands: Dordrecht, 2016; pp. 1–11 ISBN 978-94-007-6172-8.
2. *Encyclopedia of Coastal Science*; Ritchie, W., Ed.; Encyclopedia of Earth Sciences Series; Springer International Publishing, 2019; ISBN 978-3-319-93805-9.
3. Abiye, T. The Role of Wetlands Associated to Urban Micro-Dams in Pollution Attenuation, Johannesburg, South Africa. *Wetlands* **2015**, *35*, 1127–1136, doi:10.1007/s13157-015-0700-0.
4. Marotta, H.; Bento, L.; Esteves, F. de A.; Enrich-Prast, A. Whole Ecosystem Evidence of Eutrophication Enhancement by Wetland Dredging in a Shallow Tropical Lake. *Estuaries Coasts* **2009**, *32*, 654–660, doi:10.1007/s12237-009-9152-1.
5. Palmer-Felgate, E.J.; Acreman, M.C.; Verhoeven, J.T.; Scholz, M.; Maltby, E.; Stratford, C.J.; Newman, J.; Miller, J.; Coughlin, D. How Effective Are Reedbeds, Ponds, Restored and Constructed Wetlands at Retaining Nitrogen, Phosphorus and Suspended Sediment from Agricultural Pollution in England? *Environ. Evid.* **2013**, *2*, 1, doi:10.1186/2047-2382-2-1.
6. Sok, T.; Oeurng, C.; Kaing, V.; Sauvage, S.; Lu, X.; Pérez, J.M.S. Nutrient Transport and Exchange between the Mekong River and Tonle Sap Lake in Cambodia. *Ecol. Eng.* **2022**, *176*, 1645–1651, doi:10.1016/j.ecoleng.2021.106527.
7. Rao, K.; Zhang, X.; Yi, X.-J.; Li, Z.-S.; Wang, P.; Huang, G.-W.; Guo, X.-X. Interactive Effects of Environmental Factors on Phytoplankton Communities and Benthic Nutrient Interactions in a Shallow Lake and Adjoining Rivers in China. *Sci. Total Environ.* **2018**, *619–620*, 1661–1672, doi:10.1016/j.scitotenv.2017.10.135.
8. Chang, N.-B.; Imen, S.; Vannah, B. Remote Sensing for Monitoring Surface Water Quality Status and Ecosystem State in Relation to the Nutrient Cycle: A 40-Year Perspective. *Crit. Rev. Environ. Sci. Technol.* **2015**, *45*, 101–166, doi:10.1080/10643389.2013.829981.
9. Jia, Z.; Chang, X.; Duan, T.; Wang, X.; Wei, T.; Li, Y. Water Quality Responses to Rainfall and Surrounding Land Uses in Urban Lakes. *J. Environ. Manage.* **2021**, *298*, 113514, doi:10.1016/j.jenvman.2021.113514.
10. Nausch, M.; Woelk, J.; Kahle, P.; Nausch, G.; Leipe, T.; Lennartz, B. Phosphorus Fractions in Discharges from Artificially Drained Lowland Catchments (Warnow River, Baltic Sea). *Agric. Water Manag.* **2017**, *187*, 77–87, doi:10.1016/j.agwat.2017.03.006.
11. Nikolaidis, N.P.; Phillips, G.; Poikane, S.; Várbíró, G.; Bouraoui, F.; Malagó, A.; Lilli, M.A. River and Lake Nutrient Targets That Support Ecological Status: European Scale Gap Analysis and Strategies for the Implementation of the Water Framework Directive. *Sci. Total Environ.* **2022**, *813*, 151898, doi:10.1016/j.scitotenv.2021.151898.
12. Zheng, Z.; Xu, Y.; Wang, J.; Li, Y.; Gu, B. Environmental Stress and Eutrophication in Freshwater Wetlands: Evidence from Carbon and Nitrogen Stable Isotopes in Cattail (Typha Domingensis Pers.). *Ecol. Process.* **2019**, *8*, 1–8, doi:10.1186/S13717-019-0186-4/TABLES/4.
13. Wang, Q.; Rogers, M.J.; Ng, S.S.; He, J. Fixed Nitrogen Removal Mechanisms Associated with Sulfur Cycling in Tropical Wetlands. *Water Res.* **2021**, *189*, 116619, doi:10.1016/j.watres.2020.116619.

14. Hes, E.MA.; van Dam, A.A. Modelling Nitrogen and Phosphorus Cycling and Retention in Cyperus Papyrus Dominated Natural Wetlands. *Environ. Model. Softw.* **2019**, *122*, 104531, doi:10.1016/j.envsoft.2019.104531.
15. Li, H.; Ma, X.; Zhou, B.; Ren, G.; Yuan, D.; Liu, H.; Wei, Z.; Gu, X.; Zhao, B.; Hu, Y.; et al. An Integrated Migration and Transformation Model to Evaluate the Occurrence Characteristics and Environmental Risks of Nitrogen and Phosphorus in Constructed Wetland. *Chemosphere* **2021**, *277*, 130219, doi:10.1016/j.chemosphere.2021.130219.
16. Campo-Daza, G.A.; Zumaqué, L.; Torres-Bejarano, F.M. Efficiency Assessment of Constructed Wetlands for Fuel Contaminated Water Treatment. *Int. J. Environ. Sci. Technol.* **2021**, *19*, 12, doi:10.1007/s13762-021-03901-2.
17. González-Márquez, L.C.; Torres-Bejarano, F.M.; Rodríguez-Cuevas, C.; Torregroza-Espinosa, A.C.; Sandoval-Romero, J.A. Estimation of Water Quality Parameters Using Landsat 8 Images: Application to Playa Colorada Bay, Sinaloa, Mexico. *Appl. Geomat.* **2018**, *10*, 147–158, doi:10.1007/s12518-018-0211-9.
18. Elsayed, S.; Ibrahim, H.; Hussein, H.; Elsherbiny, O.; Elmetwalli, A.H.; Moghanm, F.S.; Ghoneim, A.M.; Danish, S.; Datta, R.; Gad, M. Assessment of Water Quality in Lake Qaroun Using Ground-Based Remote Sensing Data and Artificial Neural Networks. *Water* **2021**, *13*, 3094, doi:10.3390/w13213094.
19. Germán, A.; Shimoni, M.; Beltramone, G.; Rodríguez, M.I.; Muchiut, J.; Bonansea, M.; Scavuzzo, C.M.; Ferral, A. Space-Time Monitoring of Water Quality in an Eutrophic Reservoir Using SENTINEL-2 Data - A Case Study of San Roque, Argentina. *Remote Sens. Appl. Soc. Environ.* **2021**, *24*, 100614, doi:10.1016/j.rsase.2021.100614.
20. Momen, B.; Eichler, L.W.; Boylen, C.W.; Zehr, J.P. Application of Multivariate Statistics in Detecting Temporal and Spatial Patterns of Water Chemistry in Lake George, New York. *Ecol. Model.* **1996**, *91*, 183–192, doi:10.1016/0304-3800(95)00189-1.
21. Mattikalli, N.M.; Richards, K.S. Estimation of Surface Water Quality Changes in Response to Land Use Change: Application of The Export Coefficient Model Using Remote Sensing and Geographical Information System. *J. Environ. Manage.* **1996**, *48*, 263–282, doi:10.1006/jema.1996.0077.
22. Wu, C.; Wu, J.; Qi, J.; Zhang, L.; Huang, H.; Lou, L.; Chen, Y. Empirical Estimation of Total Phosphorus Concentration in the Mainstream of the Qiantang River in China Using Landsat TM Data. *Int. J. Remote Sens.* **2010**, *31*, 2309–2324, doi:10.1080/01431160902973873.
23. Al-Shaibah, B.; Liu, X.; Zhang, J.; Tong, Z.; Zhang, M.; El-Zeiny, A.; Faichia, C.; Hussain, M.; Tayyab, M. Modeling Water Quality Parameters Using Landsat Multispectral Images: A Case Study of Erlong Lake, Northeast China. *Remote Sens.* **2021**, *13*, 1603, doi:10.3390/rs13091603.
24. Deutsch, E.S.; Alameddine, I.; El-Fadel, M. Monitoring Water Quality in a Hypereutrophic Reservoir Using Landsat ETM+ and OLI Sensors: How Transferable Are the Water Quality Algorithms? *Environ. Monit. Assess.* **2018**, *190*, 141, doi:10.1007/s10661-018-6506-9.
25. González-Márquez, L.C.; Torres-Bejarano, F.M.; Torregroza-Espinosa, A.C.; Hansen-Rodríguez, I.R.; Rodríguez-Gallegos, H.B. Use of LANDSAT 8 Images for Depth and Water Quality Assessment of El Guájaro Reservoir, Colombia. *J. South Am. Earth Sci.* **2018**, *82*, doi:10.1016/j.jsames.2018.01.004.
26. Olmanson, L.G.; Bauer, M.E.; Brezonik, P.L. A 20-Year Landsat Water Clarity Census of Minnesota's 10,000 Lakes. *Remote Sens. Environ.* **2008**, *112*, 4086–4097, doi:10.1016/j.rse.2007.12.013.
27. Robert, E.; Grippa, M.; Kergoat, L.; Pinet, S.; Gal, L.; Cochonneau, G.; Martinez, J.-M. Monitoring Water Turbidity and Surface Suspended Sediment Concentration of the Bagre Reservoir (Burkina Faso) Using MODIS and Field Reflectance Data. *Int. J. Appl. Earth Obs. Geoinformation* **2016**, *52*, 243–251, doi:10.1016/j.jag.2016.06.016.
28. Torregroza-Espinosa, A.C.; Restrepo, J.C.; Correa-Metrio, A.; Hoyos, N.; Escobar, J.; Pierini, J.; Martínez, J.-M. Fluvial and Oceanographic Influences on Suspended Sediment Dispersal in the Magdalena River Estuary. *J. Mar. Syst.* **2020**, *204*, 103282, doi:10.1016/j.jmarsys.2019.103282.

29. Maciel, D.A.; Barbosa, C.C.F.; Novo, E.M.L. de M.; Flores Júnior, R.; Begliomini, F.N. Water Clarity in Brazilian Water Assessed Using Sentinel-2 and Machine Learning Methods. *ISPRS J. Photogramm. Remote Sens.* **2021**, *182*, 134–152, doi:10.1016/j.isprsjprs.2021.10.009.
30. Sòria-Perpinyà, X.; Vicente, E.; Urrego, P.; Pereira-Sandoval, M.; Ruíz-Verdú, A.; Delegido, J.; Soria, J.M.; Moreno, J. Remote Sensing of Cyanobacterial Blooms in a Hypertrophic Lagoon (Albufera of València, Eastern Iberian Peninsula) Using Multitemporal Sentinel-2 Images. *Sci. Total Environ.* **2020**, *698*, 134305, doi:10.1016/j.scitotenv.2019.134305.
31. Torres-Bejarano, F.M.; Arteaga-Hernández, F.; Rodríguez-Ibarra, D.; Mejía-Ávila, D.; González-Márquez, L.C. Water Quality Assessment in a Wetland Complex Using Sentinel 2 Satellite Images. *Int. J. Environ. Sci. Technol.* **2021**, *18*, 2345–2356, doi:10.1007/s13762-020-02988-3.
32. Casal, G. Assessment of Sentinel-2 to Monitor Highly Dynamic Small Water Bodies: The Case of Louro Lagoon (Galicia, NW Spain). *Oceanologia* **2022**, *64*, 88–102, doi:10.1016/j.oceano.2021.09.004.
33. Petus, C.; Waterhouse, J.; Lewis, S.; Vacher, M.; Tracey, D.; Devlin, M. A Flood of Information: Using Sentinel-3 Water Colour Products to Assure Continuity in the Monitoring of Water Quality Trends in the Great Barrier Reef (Australia). *J. Environ. Manage.* **2019**, *248*, 109255, doi:10.1016/j.jenvman.2019.07.026.
34. Mortula, M.; Ali, T.; Bachir, A.; Elaksher, A.; Abouleish, M. Towards Monitoring of Nutrient Pollution in Coastal Lake Using Remote Sensing and Regression Analysis. *Water* **2020**, *12*, 1954, doi:10.3390/w12071954.
35. Torregroza-Espinosa, A.C.; Restrepo, J.C.; Escobar, J.; Brenner, M.; Newton, A. Nutrient Inputs and Net Ecosystem Productivity in the Mouth of the Magdalena River, Colombia. *Estuar. Coast. Shelf Sci.* **2020**, *243*, 106899, doi:10.1016/j.ecss.2020.106899.
36. Bonansea, M.; Ledesma, M.; Bazán, R.; Ferral, A.; German, A.; O'Mill, P.; Rodriguez, C.; Pinotti, L. Evaluating the Feasibility of Using Sentinel-2 Imagery for Water Clarity Assessment in a Reservoir. *J. South Am. Earth Sci.* **2019**, *95*, 102265, doi:10.1016/j.jsames.2019.102265.
37. Isenstein, E.M.; Park, M.-H. Assessment of Nutrient Distributions in Lake Champlain Using Satellite Remote Sensing. *J. Environ. Sci.* **2014**, *26*, 1831–1836, doi:10.1016/j.jes.2014.06.019.